Electrochemical and Solid-State Letters, **11** (3) H55-H59 (2008)
1099-0062/2007/11(3)/H55/5/$23.00 © The Electrochemical Society

Effect of N_2O Plasma Treatment on the Performance of ZnO TFTs

K. Remashan,[a] D. K. Hwang,[b] S. D. Park,[c] J. W. Bae,[c] G. Y. Yeom,[c] S. J. Park,[b] and J. H. Jang[a,z]

[a]*Department of Information and Communications, and* [b]*Department of Materials Science and Engineering, Gwangju Institute of Science and Technology, Gwangju 500-712, South Korea*
[c]*Department of Materials Science and Engineering, Sungkyunkwan University, Suwon, Kyunggi-do 440-746, South Korea*

Postfabrication rapid thermal annealing (RTA) and subsequent nitrous oxide (N_2O) plasma treatment improved the performance of zinc oxide (ZnO) thin-film transistors (TFTs) in terms of off current and on/off current ratio by almost 2 orders of magnitude. The off current of 2×10^{-8} A and on/off current ratio of 3×10^3 obtained after RTA were improved to 10^{-10} A and 10^5, respectively, by the subsequent N_2O plasma treatment. X-ray photoelectron spectroscopy analysis of the TFT samples showed that the RTA-treated ZnO surface had more oxygen vacancies as compared to as-deposited samples, and the oxygen vacancies at the surface of RTA-treated ZnO were reduced by subsequent N_2O plasma treatment. The reduction of oxygen vacancies at the top region of the ZnO channel is the cause of better off current and on/off current ratio of the TFTs.
© 2007 The Electrochemical Society. [DOI: 10.1149/1.2822885] All rights reserved.

Manuscript submitted October 4, 2007; revised manuscript received November 4, 2007.
Available electronically December 27, 2007.

Zinc oxide (ZnO), with a direct bandgap energy of 3.37 eV, is one of the semiconductor materials well suited for transparent thin-film transistors (TFTs) in the application areas of active matrix liquid crystal displays (AMLCDs) and electronic papers.[1-10] However, there are some technical challenges to overcome to achieve manufacturability of ZnO-based TFTs. One of the problems facing ZnO-based TFTs is high off current (leakage current) and hence low on/off current ratio.[5-9] Low off current as well as on/off current ratio higher than 10^6 are required for the ZnO TFTs to function as select transistors in AMLCDs.[10] In TFTs with bottom-gate configuration, the drain-to-source current flow through the undepleted channel region as well as the gate-leakage current contribute to the off current. To eliminate the undesired drain-to-source current under the off condition, thinner channel layers have been employed in TFTs.[2,4] However, the crystalline quality of the ZnO materials improves with thickness, so the thinner ZnO channel tends to have more defects, which affects the carrier mobility and subthreshold slope of devices.[1,6] In this work, we studied the effect of postfabrication rapid thermal annealing (RTA) and subsequent nitrous oxide (N_2O) plasma treatment on the off current and on/off current ratio of the fabricated bottom-gated ZnO TFTs. We found that the TFTs subjected to N_2O plasma treatment exhibit better off current and on/off current ratio. X-ray photoelectron spectroscopy (XPS) analysis was performed to examine the surface modification of ZnO channel layer due to RTA and N_2O plasma treatment.

Corning 1737 glass coated with 200 nm thick indium tin oxide (ITO) was used as starting substrates (sheet resistance = 4–8 Ω/□, Delta Technologies limited, USA) for fabricating TFTs with bottom-gate configuration, and the ITO acted as the gate electrode. The substrates were ultrasonically cleaned with acetone, methanol, and deionized water. ITO gate electrodes were defined by standard photolithography and wet-etching process using LCE–12k (ITO etchant, Cyantek Corporation) at 45°C. Next, a 200 nm thick silicon nitride gate-dielectric layer was deposited by plasma-enhanced chemical vapor deposition (PECVD) using SiH_4, NH_3, and N_2 gases with the growth parameters $SiH_4/NH_3/N_2$ = 400/20/600 sccm, pressure = 650 mTorr, power = 30 W, and temperature = 300°C. A 250 nm thick ZnO channel layer was then deposited by radio frequency (rf) magnetron sputtering using a commercially available undoped ZnO target (PureTech) at 350°C. The sputtering was performed in a mixed ambient of O_2 and Ar (Ar/O_2 gas flow ratio = 1/3) with an rf power of 100 W and working pressure of 4 mTorr. The structure of the ZnO film was found to be polycrystalline by X-ray diffraction measurement.[11] Hall mobility and carrier concentration of the grown undoped ZnO channel layer could not be measured using the Hall measurement system due to its high electrical resistivity. The grown ZnO was subsequently patterned by conventional photolithography and etching process using $HCl:HNO_3:H_2O$ (4:1:200). Source and drain contacts comprising Ti/Pt/Au (20/30/150 nm) were deposited by e-beam evaporation. Finally, vias for contact to the gate electrode were established by photolithography and dry etching of silicon nitride with CF_4/O_2 gas mixtures. The schematic cross-sectional view and the scanning electron microscopy (SEM) top view of the fabricated TFTs are shown in Fig. 1a and b, respectively. The channel width (W) and channel length (L) of the TFTs are 200 and 20 μm, respectively. The fabricated devices were subjected to RTA and N_2O plasma treatment to improve their performances. RTA was performed at 270°C, and the subsequent N_2O plasma treatment was carried out at two different temperatures, such as 200 and 250°C. For comparison purposes, the RTA-treated TFTs were also subjected to N_2 plasma treatment instead of N_2O. The electrical characteristics of the TFTs were measured using a semiconductor parameter analyzer (HP 4155 A).

The as-fabricated TFTs exhibited currents only in the picoampere range due to low electron concentration in the ZnO channel layer. In order to increase conductivity of ZnO channel and to obtain better current level, annealing of ZnO TFTs under N_2 ambient[9,12,13] as well as under forming gas ambient[9,12,14] has been reported. To increase resistivity of the ZnO samples, annealing under oxygen ambient[1,15] has been reported. In the present case, postfabrication annealing of the fabricated ZnO TFTs was performed in the N_2 ambient to increase conductivity of ZnO films, resulting in a drain current in the microampere range. The output characteristics (I_D-V_{DS}) and transfer characteristics (I_D-V_{GS}) of the TFTs after RTA at 270°C for 5 min in N_2 ambient are shown in Fig. 2a and b, respectively. From Fig. 2a, good current saturation and on current of about 55 μA at the bias condition ($V_{GS} = V_{DS} = 40$ V) are observed. The field-effect mobility (μ_{FE}) of polycrystalline ZnO TFTs operating in saturation region can be extracted using the following current equation[13]

$$I_D = \frac{1}{2} C_i \mu_{FE} \frac{W}{L} (V_{GS} - V_T)^2 \quad [1]$$

where C_i is the gate capacitance per unit area of the gate insulator and V_T is the threshold voltage. The estimated μ_{FE} of the TFTs is 0.88 cm^2/V s. The subthreshold slope (S) of TFTs is usually extracted from their transfer characteristics in the subthreshold regime using the following equation

[z] E-mail: jjang@gist.ac.kr

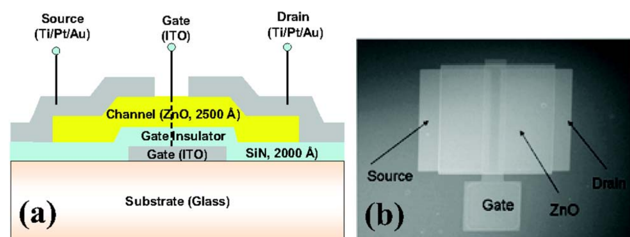

Figure 1. (Color online) The fabricated ZnO-based TFTs: (a) schematic cross-sectional view and (b) SEM top view.

$$S = \frac{dV_{GS}}{d(\log I_D)} \quad [2]$$

The extracted subthreshold slope is 10.5 V/decade in the current region between 10^{-7} and 10^{-6} A. From the transfer characteristics shown in Fig. 2b, it can be seen that the off current is about 10^{-8} A and the on/off current ratio is only about 3×10^3. As the gate current is only about 10^{-10} A as shown in Fig. 2b, the off current is not limited by the gate-leakage current but by the current flow in the undepleted region of the ZnO channel near the top surface. As oxygen vacancies act as shallow n-type dopants in ZnO materials,[9,16] creation of oxygen vacancies can be responsible for the improved conductivity of the ZnO TFTs after the annealing. Oxygen vacancies in the undepleted channel region can be responsible for the large leakage current of 10^{-8} A observed in the RTA-treated devices. Oxygen vacancies can be reduced by subjecting the ZnO TFTs to high-temperature annealing in the oxygen ambient.[1,15] Here, we used N_2O plasma at relatively low temperatures to reduce oxygen vacancies. In order to see the influence of N_2O plasma treatment on the off current, the annealed TFTs were subjected to N_2O plasma in a PECVD chamber at two different temperatures of 200 and 250°C. The N_2O plasma treatment conditions, i.e., the chamber pressure, rf power, and N_2O flow rate, were 300 mTorr, 20 W, and 300 sccm, respectively. The N_2O plasma treatment at 200°C was carried out for 1, 3, and 5 min, while the N_2O treatment at 250°C was performed for 5 min. The transfer characteristics and gate-leakage currents of the N_2O-treated TFTs at 200°C for three different durations are shown in Fig. 3a. The output and transfer characteristics obtained after the 5 min N_2O treatment are shown in Fig. 3b and c, respectively. In this case, the extracted μ_{FE} of the TFTs is 0.36 cm^2/V s. The subthreshold slope is 10.5 V/decade in the current range of 10^{-7}–10^{-6} A, and that in the current range of 10^{-8}–10^{-7} A is 7.5 V/decade. As shown in Fig. 3a, the off current is dependent on the N_2O plasma treatment time. The off current continuously decreases with increasing treatment time, and finally the off current of the TFTs after 5 min N_2O treatment is limited by the gate-leakage current by successfully eliminating the drain-to-source leakage current. With 5 min N_2O treatment, the off current dropped by about 2 orders of magnitude and the on/off current ratio was improved to higher than 10^5. The improvement in the off current can be ascribed to the reduction of oxygen vacancies in the undepleted region at the top surface of the channel. From Fig. 3a, it can be observed that the on current also decreased with N_2O plasma treatment time. However, the reduction of on current is much lower as compared to that of the off current. The on current reduction can be explained as follows. The oxygen incorporation during N_2O plasma treatment may not be happening only at the surface region of the channel. The incorporated oxygen may also diffuse into the channel and thereby reduce the effective carrier concentration within the channel. This argument for on-current reduction can be more convincing if we look at the output characteristics of the TFTs after N_2O plasma treatment at a slightly higher temperature of 250°C for 5 min, as shown in Fig. 4. It can be seen from Fig. 4 that the on current is in the nanoampere range. The reduction of on current from microampere range (Fig. 2a) to nanoampere range (Fig. 4a) as a result of N_2O plasma treatment can be ascribed to reduction of carrier concentration in the ZnO layer due to incorporation of large amounts of oxygen during the plasma treatment. The improvement of the off current as well as the reduction of on current can be attributed to the incorporation of oxygen into the ZnO layer from the N_2O plasma. Because oxygen vacancies in ZnO material act as n-type dopants,[9,16] the reduction of oxygen vacancies can decrease the carrier concentration at the top region of the channel, which results in low off current. The results of XPS studies (described later in this paper) carried out on the TFT samples indeed support our argument on the off current and on current reductions. P-type semiconductor properties have been reported in nitrogen-doped zinc oxide,[17] and incorporation of nitrogen into the ZnO region can also affect the off current of TFTs. In the present case, therefore, to see if nitrogen from N_2O plasma is playing any role in the improvement of

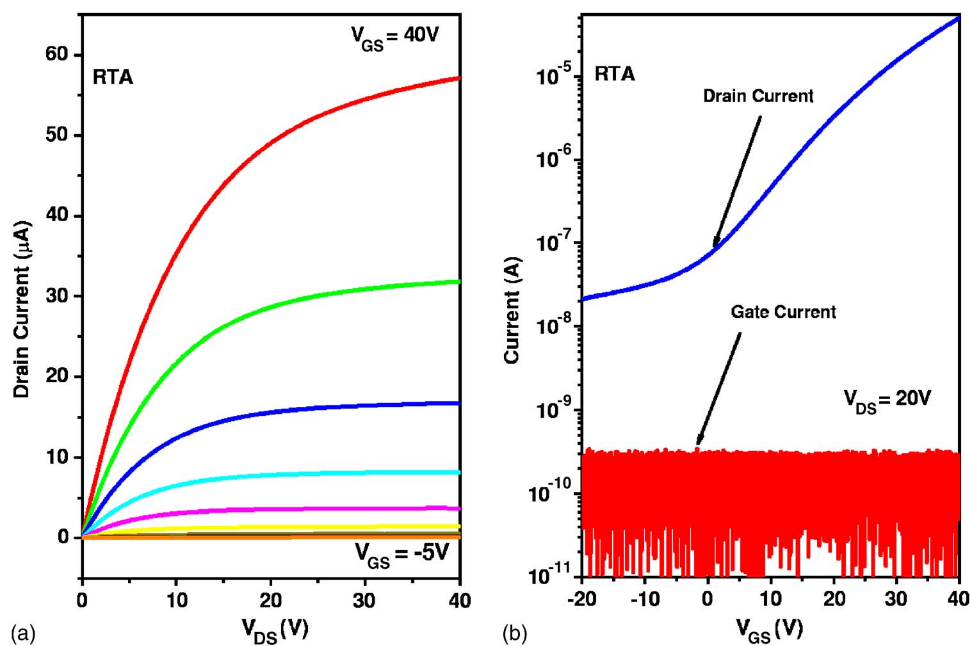

Figure 2. (Color online) Characteristics of ZnO TFTs after RTA at 270°C for 5 min in N_2 ambient: (a) output characteristics with V_{GS} from 40 to − 5 V in steps of −5 V and (b) transfer characteristics and gate-leakage current at V_{DS} = 20 V.

Figure 3. (Color online) Characteristics of ZnO TFTs after the combined treatment of RTA at 270°C for 5 min in N_2 ambient and N_2O plasma treatment at 200°C: (a) transfer characteristics for different N_2O plasma treatment times (0, 1, 3, and 5 min) at V_{DS} = 20 V, (b) output characteristics with V_{GS} from 40 to 10 V in steps of −5 V, after 5 min N_2O plasma treatment, and (c) transfer characteristics and gate-leakage current at V_{DS} = 20 V, after N_2O plasma treatment for 5 min.

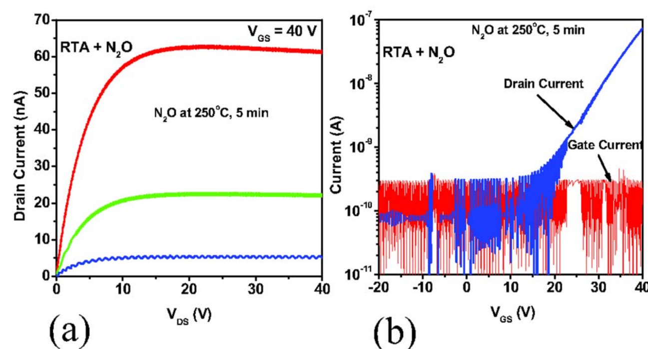

Figure 4. (Color online) Characteristics of ZnO TFTs after the combined treatment of RTA at 270°C for 5 min in N_2 ambient and N_2O plasma treatment at 250°C for 5 min: (a) output characteristics with V_{GS} from 40 to 30 V in steps of −5 V and (b) transfer characteristics and gate-leakage current at V_{DS} = 20 V.

on/off current ratio, one set of TFTs was subjected to N_2 plasma under the same N_2O plasma conditions (200°C for 5 min). The transfer characteristics of the TFTs obtained before and after the N_2 plasma treatment are shown in Fig. 5. It can be seen from Fig. 5 that the TFTs exhibit essentially the same characteristics, which suggests that the better on/off current ratio obtained after N_2O plasma treatment is not due to nitrogen doping but to the presence of oxygen.

In order to examine the cause of the better off current and on/off current ratio obtained after N_2O plasma treatment, XPS analysis was carried out on the ZnO samples. XPS measurements were performed using a MultiLab 2000 X-ray photoelectron spectrometer (Thermo Electron Corporation, USA) with Mg Kα X-ray source ($h\nu$ = 1253.60 eV). The samples used for the XPS study have the same layer structure as those used for fabricating TFTs. Three sets of samples, namely, as-deposited samples, RTA-treated samples at 270°C for 5 min, and samples subjected to the combined processing of RTA (270°C for 5 min) and N_2O (200°C for 5 min) treatments, were analyzed using XPS. The energy of the XPS signals was shifted due to electrostatic charging caused by the use of an insulating glass substrate, and the binding energies of O 1s and Zn 2p were calibrated by taking the binding energy of C 1s peak as a reference in XPS. Figure 6a shows XPS spectra of O 1s on the surface of (*i*)

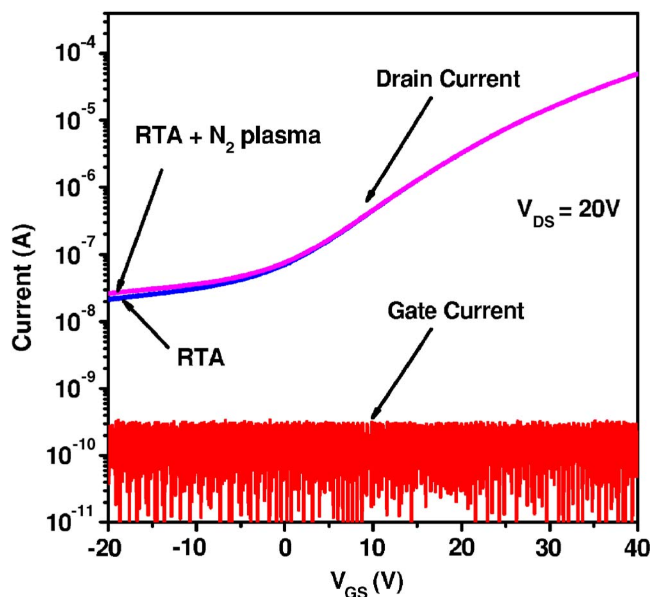

Figure 5. (Color online) Transfer characteristics and gate-leakage current at $V_{DS} = 20$ V. The ZnO TFTs were treated by RTA at 270°C for 5 min in N_2 ambient and by N_2 plasma at 200°C for 5 min.

as-grown, (*ii*) RTA treated, and (*iii*) combined RTA and N_2O-plasma-treated ZnO samples. In all cases, O 1s peaks can be deconvoluted into two peaks, as shown in Fig. 6a. The peak with the lower binding-energy component is assigned to oxygen in Zn–O bond and the other with the higher binding-energy component is assigned to oxygen loosely bound on the surface of ZnO.[18-20] In the case of the RTA-treated sample, the O 1s core-level spectrum shifted to a higher-binding-energy side by 0.53 eV compared to that of the as-grown sample. The shift of the binding energy can be due to the increase of oxygen vacancies in ZnO film that should be ionized.[18-22] In general, an ionized oxygen vacancy in ZnO film donates two electrons to the conduction band, which is mainly responsible for the conductive characteristics of ZnO films.[16] The increased electron density due to the ionized oxygen vacancies move the Fermi level up closer to the conduction band, which results in the decrease of work function. This appeared to be the reason why

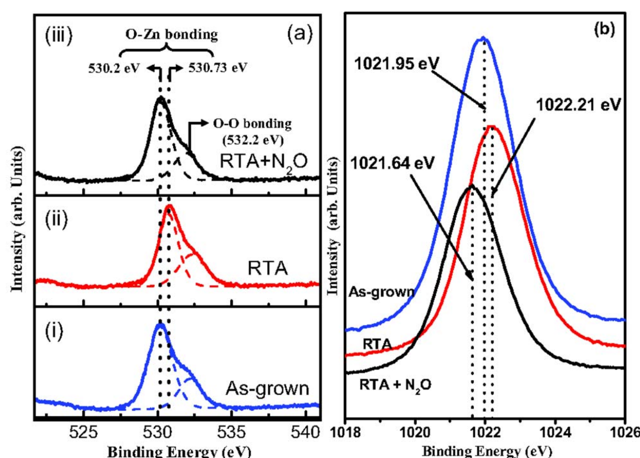

Figure 6. (Color online) XPS spectra obtained on the as-deposited samples, RTA-treated samples, and samples treated with both RTA and N_2O: (a) O 1s spectra and (b) Zn $2p_{3/2}$ spectra.

Table I. Atomic percentages of oxygen in Zn–O bond and loosely bound on the surface of ZnO films for three different cases.

	As-grown (%)	RTA (%)	RTA + N_2O (%)
Zn–O	71.53	62.36	71.83
O–O	28.47	37.64	28.17

the O 1s peak shifted toward the higher-binding-energy side in the XPS spectrum. After the combined process of RTA and N_2O plasma treatments, the O 1s peak moved to a lower-binding-energy position at 530.20 eV, which coincides with that obtained on the as-grown sample. This shows that the combined treatment brings the sample surface condition back to that of the as-deposited sample. The electrical characteristics of the as-fabricated and the RTA + N_2O-treated TFTs are shown in Fig. 7. The on currents are in the nanoampere and microampere range for the as-fabricated and the RTA + N_2O-treated TFTs, respectively. From Fig. 7c, it is clear that the TFTs have the same off current. These results show the effectiveness of the RTA + N_2O treatment in improving the on/off current ratio of TFTs. From the results of XPS analyses, the normalized atomic percentages of oxygen in Zn–O bond are 71.5, 62.4, and 71.8% for as-grown, RTA-treated, and RTA + N_2O-treated samples, respectively, as shown in Table I. The decreased atomic percentage of oxygen in Zn–O bond in the RTA-treated sample indicates that the ionized oxygen vacancies are increased in the RTA-treated sample. The atomic percentage of oxygen in Zn–O bond of the RTA + N_2O-treated sample returned to that of the as-grown sample, which shows that the oxygen vacancies are decreased at the surface of this sample. Therefore, the higher off current observed in the electrical characteristics of TFTs subjected to RTA can be ascribed to the increased ionized oxygen vacancies near the top surface of the TFTs. During the N_2O plasma treatment, oxygen enters ZnO and reduces the oxygen vacancies at the top surface of the ZnO and thereby decreases the off current. However, XPS can only analyze the surface of ZnO film, and the off current cannot be attributed only to the surface current flow. The off current can also be contributed by the current flow beneath the top surface. It is difficult to get accurate depth profiles from XPS due to surface modification of oxide-related materials during the sputtering process. More experimental work is required to extract the thickness of the film which is influenced (oxidized) by the N_2O plasma treatment. The Zn $2p_{3/2}$ spectra on the surface of the (*i*) as-grown, (*ii*) RTA-treated, and (*iii*) combined-treated RTA and N_2O samples are shown in Fig. 6b. The as-grown sample shows a Zn peak at 1021.95 eV, and this peak corresponds to crystal lattice zinc from ZnO.[18,19,23,24] After RTA, the Zn peak moved to a higher-binding-energy position at 1022.21 eV, which is ascribed to the zinc-enrichment situation.[19,23,24] The joint treatment of RTA and N_2O plasma moves the peak position to a lower binding energy at 1021.64 eV, i.e., the sample surface condition moves closer to that of the as-deposited samples.

In summary, postfabrication N_2O plasma treatment improved the off current and on/off current ratio of the ZnO TFTs by nearly 2 orders of magnitude. The off current of the TFTs decreased from 2×10^{-8} to 10^{-10} A and the on/off current ratio increased from 3×10^3 to 10^5. From XPS studies, it was concluded that oxygen present in the N_2O modified the top region of the ZnO channel layer during the N_2O plasma treatment. Oxygen vacancies, which act as n-type dopants in ZnO materials, near the top region of the ZnO were reduced by N_2O plasma treatment, resulting in low off current and high on/off current ratio.

Acknowledgments

This work was financially supported by KOSEF (grant no. R01-2007-000-10843-0), MOCT, and KICTTEP through SEAHERO program.

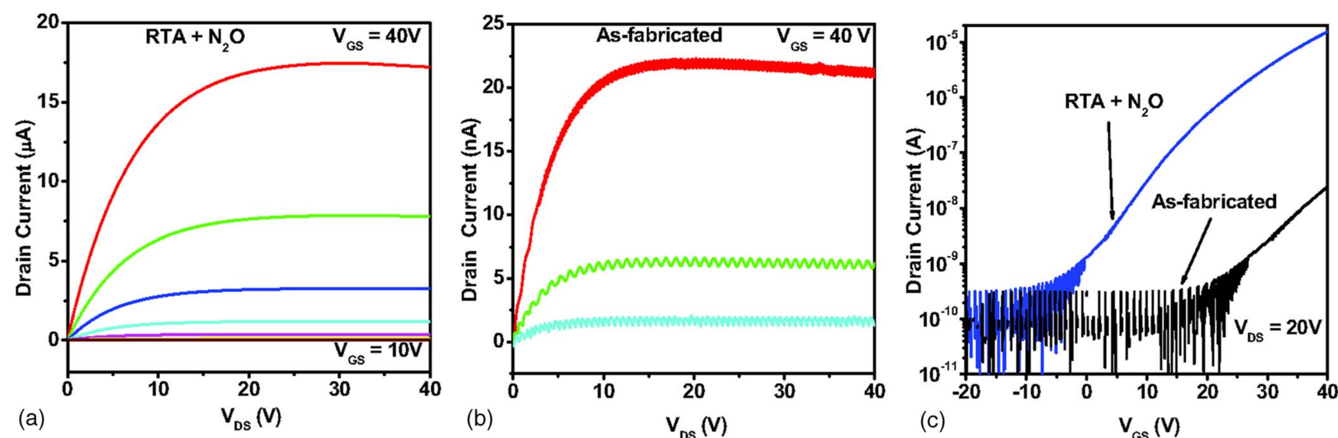

Figure 7. (Color online) (a) Output characteristics of ZnO TFTs with V_{GS} from 40 to 10 V in steps of −5 V after RTA (270°C, 5 min) and N_2O plasma treatment (200°C, 5 min), (b) output characteristics of as-fabricated TFTs with V_{GS} from 40 to 30 V in steps of −5 V, and (c) transfer characteristics of as-fabricated and RTA + N_2O (200°C, 5 min)-treated TFTs at V_{DS} = 20 V.

Gwangju Institute of Science and Technology assisted in meeting the publication costs of this article.

References

1. D. Redinger and V. Subramanian, *IEEE Trans. Electron Devices*, **54**, 1301 (2007).
2. M. H. Lim, K. T. Kang, H. G. Kim, I. D. Kim, Y. W. Choi, and H. L. Tuller, *Appl. Phys. Lett.*, **89**, 202908 (2006).
3. R. Navamathavan, E. J. Yang, J. H. Lim, D. K. Hwang, J. Y. Oh, J. H. Jang, and S. J. Park, *J. Electrochem. Soc.*, **153**, G385 (2006).
4. H. H. Hsieh and C. C. Wu, *Appl. Phys. Lett.*, **91**, 013502 (2006).
5. C. C. Liu, Y. S. Chen, and J. J. Huang, *Electron. Lett.*, **42**, 824 (2006).
6. B. Y. Oh, M. C. Jeong, M. H. Ham, and J. M. Myoung, *Semicond. Sci. Technol.*, **22**, 608 (2007).
7. K. T. Kang, M. H. Lim, and H. G. Kim, *Appl. Phys. Lett.*, **90**, 043502 (2007).
8. P. F. Carcia, R. S. McLean, and M. H. Reilly, *Appl. Phys. Lett.*, **88**, 123509 (2006).
9. H. S. Bae, J. H. Kim, and S. Im, *Electrochem. Solid-State Lett.*, **7**, G279 (2004).
10. J. F. Wager, *Science*, **300**, 1245 (2003).
11. R. Navamathavan, J. H. Lim, D. K. Hwang, B. H. Kim, J. Y. Oh, J. H. Jang, H. S. Kim, and S. J. Park, *J. Korean Phys. Soc.*, **48**, 271 (2006).
12. H. S. Bae and S. Im, *J. Vac. Sci. Technol. B*, **22**, 1191 (2004).
13. H. H. Hsieh and C. C. Wu, *Appl. Phys. Lett.*, **89**, 041109 (2006).
14. I. D. Kim, Y. W. Choi, and H. L. Tuller, *Appl. Phys. Lett.*, **87**, 043509 (2005).
15. R. L. Hoffman, N. Norris, and J. F. Wager, *Appl. Phys. Lett.*, **82**, 733 (2003).
16. Y. Ma, G. T. Du, T. P. Yang, D. L. Qiu, X. Zhang, H. J. Yang, Y. T. Zhang, B. J. Zhao, X. T. Yang, and D. L. Liu, *J. Cryst. Growth*, **255**, 303 (2003).
17. B. Yao, D. Z. Shen, Z. Z. Zhang, X. H. Wang, Z. P. Wei, B. H. Li, Y. M. Lv, X. W. Fan, L. X. Guan, G. Z. Xing, et al., *J. Appl. Phys.*, **99**, 123510 (2006).
18. Z. G. Wang, X. T. Zu, S. Zhu, and L. M. Wang, *Physica E (Amsterdam)*, **35**, 199 (2006).
19. M. Chen, X. Wang, Y. H. Yu, Z. L. Pei, X. D. Bai, C. Sun, R. F. Huang, and L. S. Wen, *Appl. Surf. Sci.*, **158**, 134 (2000).
20. T. Szorenyi, L. D. Laude, I. Bertoti, Z. Kantor, and Z. G. Vszky, *J. Appl. Phys.*, **78**, 6211 (1995).
21. C. C. Lin, H. P. Chen, H. C. Liao, and S. Y. Chen, *Appl. Phys. Lett.*, **86**, 183103 (2005).
22. J. C. C. Fan and J. B. Goodenough, *J. Appl. Phys.*, **48**, 3524 (1977).
23. Y. Zhang, G. Du, X. Wang, W. Li, X. Yang, Y. Ma, B. Zhao, H. Yang, D. Liu, and S. Yang, *J. Cryst. Growth*, **252**, 180 (2003).
24. H. Li, H. Liu, J. Wang, S. Yao, X. Cheng, and R. I. Boughton, *Mater. Lett.*, **583**, 3630 (2004).